Measurement and calculation of sound transmission across junctions of solid timber building elements

Simon Mecking; Tobias Kruse; Ulrich Schanda
Laboratory for Sound Measurement LaSM, University of Applied Sciences Rosenheim, Germany.

Summary
The number of multi-storey buildings in timber construction increases continuously. Compared to concrete and brick constructions the planning process of sound insulation of a wooden building causes much higher effort. Reasons are missing planning data and planning tools for sound insulation. Suitable, computer-based tools, which enable a simulation already in an early planning phase of a building, could help to reduce the planning effort significantly. One possibility to calculate the in-situ airborne and impact sound insulation is to combine the Finite Element Method (FEM) and the Statistical Energy Analysis (SEA) in a coupled model, which consider the direct transmission path of the building elements and the flanking transmission paths. The SEA-based calculation of the sound insulation according to EN 12354 requires the vibration reduction indices of the transfer paths at a junction of structural elements. This paper shows measurement results of the Operational Vibration Analysis and the vibration reduction indices of coupled Cross Laminated Timber (CLT) elements. The influence of elastic layers, the pressure on the coupling of the elements and the fasteners was investigated. The measured results will be compared with the modeling of the junction by using a commercial SEA tool.

PACS no. 43.40.At

1. Introduction

Within the context of an efficient and sustainable design of buildings a trend towards lightweight structures, e.g. timber structures is recognizable. This trend implies the necessity to be able to predict serviceability and comfort as well as sound transmission in order to fulfil building requirements. To generate reliable prediction methods a detailed understanding of the transfer of energy between building components is compulsory.

This contribution focuses on the measurement and investigation of vibration reduction indices necessary to apply the simplified SEA approach of EN 12354. The results are a contribution to a joint research project *Vibroacoustics in the planning process for timber constructions*, which deals with the modelling of sound transmission in wooden buildings in all relevant frequency range using different computation models. An overview is given in [1].

In the low frequency range with clearly separated eigenmodes the Finite Element Method (FEM) is a convenient tool to predict the vibroacoustic behavior. The increase of the modal density with higher frequencies impedes a FEM approach, but enables the application of statistical methods like the Statistical Energy Analysis (SEA). For the SEA approach a division of the building components into different subsystems with respect to wave polarization and geometry is performed, linked with a low level of detailing. Hereby the subsystem definition is restricted to weak coupling which means (among others) that there should be only direct energetic interaction with the adjacent subsystems but not with the next but one subsystem.

The robustness of the statistical response of the SEA is achieved by averaging over time, excitation frequency and space. Hereby the choice of the frequency bandwidth is linked to the number of eigenmodes per band in order to guarantee a sufficient modal density. The modal density shows how many modes are available to store, respectively to transfer energy from one into another subsystem.

Based on the high modal density inside a subsystem it is assumed in the energetic approach that the modal energy is equivalently distributed with respect to the modes and that the modes are almost equally damped. The energy flow from one subsystem to an-

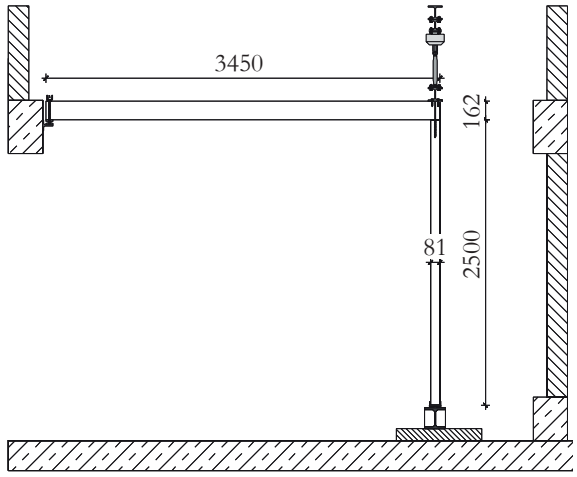

Figure 1. L*-shaped junction of wall (subsystem 2) and ceiling (subsystem 1) in the Vibroacoustics Lab.

other is proportional to the difference of the modal energies.

2. Measurements

2.1. Experimental set-up

The vibroacoustic test rig at the University at Applied Sciences in Rosenheim has been developed to carry out Operational Vibration Analyses, Power-Injection-Method and the determination of vibration reduction indices of solid timber building elements [2]. It is possible to investigate T- and L-shaped junctions of these building elements of realistic sizes with the possibility of applying an extra load of $20\,kN/m$ maximum to the junction.

For the excitation of the structure a modal shaker with a logarithmic sinus-sweep as exitation signal is used at two different positions per subsystem.

2.2. Material properties

A simplified material model for Cross Laminated Timber (CLT) has been developed in order to describe it as an orthotropic material with nine independent material parameters [3]. The modulus of elasticity has been determined by identifying the first modes and eigenfrequencies by an Operational Vibration Analysis of these panels (section 2.3). The resulting material parameters are summarized in table I.

Concerning the damping the total loss factor of each subsystem can be regarded to consist by the sum of the contribution due to material (internal) damping, friction damping, losses at junctions and radiation damping according to eq. 1 - 2. By measurement of the structural reverberation time $T_{s,j}$ of element j the total loss factor $\eta_{tot,j}$ can be determined. The direct measurement of the internal loss factor η_{jj} of these elements it is not possible. For an approximation CLT panels were hung up. By this approach the damping due to coupling losses η_{coupl} can be neglected. The radiation loss factor η_{rad} can be predicted from measured radiation efficiencies. The experiments of CLT panels in [4] have shown that η_{rad} is more than one order smaller than measured η_{tot} of hung up panels. Therefore in this experimental configuration the dominant part of the measured η_{tot} of CLT panels is the damping loss factor η_{jj}.

$$\eta_{tot,j} = \eta_{jj} + \eta_{fric} + \eta_{coupl} + \eta_{rad} \tag{1}$$

$$= \eta_{jj} + \Sigma\eta_{ji} \approx \frac{2.2}{f \cdot T_{s,j}} \tag{2}$$

2.3. Operational Vibration Analysis

The Operational Vibration Analysis was carried out to investigate the vibroacoustic behaviour in the low frequency range of the L-shaped element combination. The distances of the meshgrid were between 35 cm and 47 cm. The fineness of the meshgrid with respect to bending wavelength allows to analyse the modal behaviour up to approx. 280 Hz.

The imaginary part of the complex transfer accelerance $\underline{H_{aF}}$ (eq. 3) in equation 4 of every single point is used as amplitude $A_H(x, y, f)$ for the visualisation (s. fig. 2) of the vibroacoustic behaviour of the structure.

$$\underline{H_{aF}} = \frac{\underline{a}}{\underline{F}} \tag{3}$$

$$A_H = |\underline{H_{aF}}| \cdot sin(\phi) = \Im\left\{\underline{H_{aF}}\right\} \tag{4}$$

In the frequency range where vibration modes clearly separate, the number of modes within a certain frequency band can be determined by simply counting the peaks of the magnitude of the point accelerance. This gives a hint on the lower frequency limit where the prerequisite on modal density for an SEA is fulfilled. Whether the prerequisite of *weak coupling* is fulfilled, can be analysed by comparing the vibroacoustic behaviour of both subsystems. Figure 2 shows an example for a global mode. Subsystem 2 (wall) was exited, but due to a strong interaction the subsystem 1 (floor) is exited as well. The energy transfer has to be assumed to be very high, the requirement of weak coupling is probably not fulfilled. To answer this question requires to analyze the ratio of the vibroacoustic energy in each subsystem in terms of e.g. energy influence coefficients [6].

2.4. Vibration reduction indices

The vibration reduction indices $K_{\overline{ij}}$ in eq. 5 [7, 8] are necessary to predict sound insulation of the flanking transmission path according to the SEA approach used in EN 12354. It is calculated by the direction

Table I. Material properties of the CLT elements in fig. 3, measured at wood moisture u. [2, 5]

	E_x, E_y, E_z in N/mm^2	G_{xy}, G_{xz}, G_{yz} in N/mm^2	$\upsilon_{xy}, \upsilon_{xz}, \upsilon_{yz}$ [-]	c_L in m/s	ρ in $\frac{kg}{m^3}$	u in %
	8170	459	0.035/0.018			
Subsystem 1	2948	168	0.045/0.010	4566	455	10 ± 2
CLT with 6 layers, $z = 162\,mm$	137	103	0.037/0.020			
	10 529	459	0.035/0.018			
Subsystem 2	408	168	0.045/0.010	-	450	10 ± 2
CLT with 3 layers, $z = 81\,mm$	137	103	0.037/0.020			

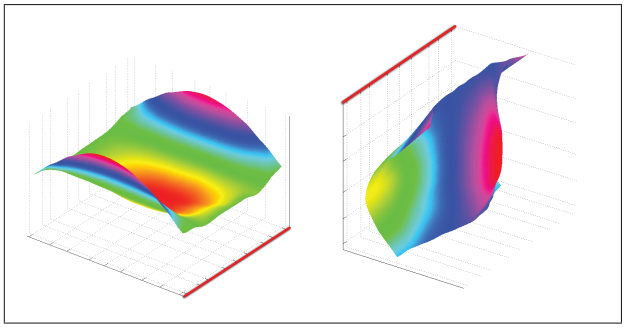

Figure 2. A global mode at $f \approx 43\,Hz$.Vibroacoustic behaviour of L-shaped junction (left: ceiling, right: wall) without interlayer (s. fig. 3, left) with an excitation point at subsystem 2 (wall). The junction line is shown in red.

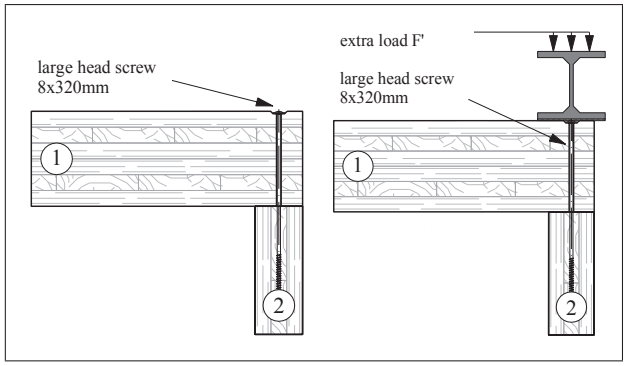

Figure 3. Variations of L-shaped junctions. In the left case (L) with one transfer path between the subsystems and in the right case (L*) with an additional transfer path, because of the extra load. The distance between two screws is 40 cm.

averaged velocity level difference $D_{v,\overline{ij}}$, the equivalent absorption length a of both subsystems, the length of the junction l_{ij} and the reference frequency $f_{ref} = 1000\,Hz$.

$$K_{\overline{ij}} = D_{v,\overline{ij}} + 10 \cdot \lg \frac{l_{ij}}{\sqrt{a_i \cdot a_j}} \tag{5}$$

$$D_{v,\overline{ij}} = \frac{D_{v,ij} + D_{v,ji}}{2} \tag{6}$$

$$a_i = \frac{\pi^2\, S_i\, \eta_{tot,i}}{c_0}\, f \sqrt{\frac{f_{ref}}{f}} \tag{7}$$

2.4.1. L-shaped junction

As an example for measured input data for the calculation of the vibration reduction index $K_{\overline{ij}}$ according to eq. 5 total loss factors of both subsystems of the L-shaped junction (s. fig. 3, left) are presented in figure 4 and the velocity level difference between both elements in figure 5. Two variations (with interlayer vs. without interlayer) of the screwd connection shows the effect of a resilient interlayer. Figure 4 indicates an increase of the total loss factor of subsystem 2 (wall) in the low frequency range, but it cannot be observed in the case of subsystem 1 (ceiling). In contrast $D_{v,\overline{12}}$ in figure 5 shows an increasing difference above $160\,Hz$ with exception of $250\,Hz$. The difference in the two directions $D_{v,12}$ and $D_{v,21}$ is due to the ratio of the mass per area $m'_1/m'_2 = 2$ [1]. The resulting vibration reduction indices in figure 6 confirm the lower sound transmission across the junction with the resilient interlayer in the mid and high frequency range.

The effect of an extra load F' on vibration reduction indices is shown in figure 7. The L*-shaped junction (s. fig. 3, right) has been supplemented with a resilient interlayer, matched to the resulting pressure on the junction. $K_{\overline{ij}}$ are marginal lower in the case of the higher pressure. This observation is compatible with earlier investigations [9].

2.4.2. T-shaped junction

The T-shaped junction has three sound transmission paths and is typical for building situations. To illustrate the spread of sound transmission across junctions effected by resilient interlayer two variations (fig. 8) have been examined.

The first junction had no resilient interlayer between the building elements and the fasteners were rigidly connected to the CLT.

The second junction had a resilient interlayer between subsystem 1 and 2 as well as between subsystem 1 and 4. Additionally the angle brackets had a resilient interlayer as well as the large head screws, which are used between subsystem 1 and 2. These kind of *softly coupled* fasteners are available at the market.

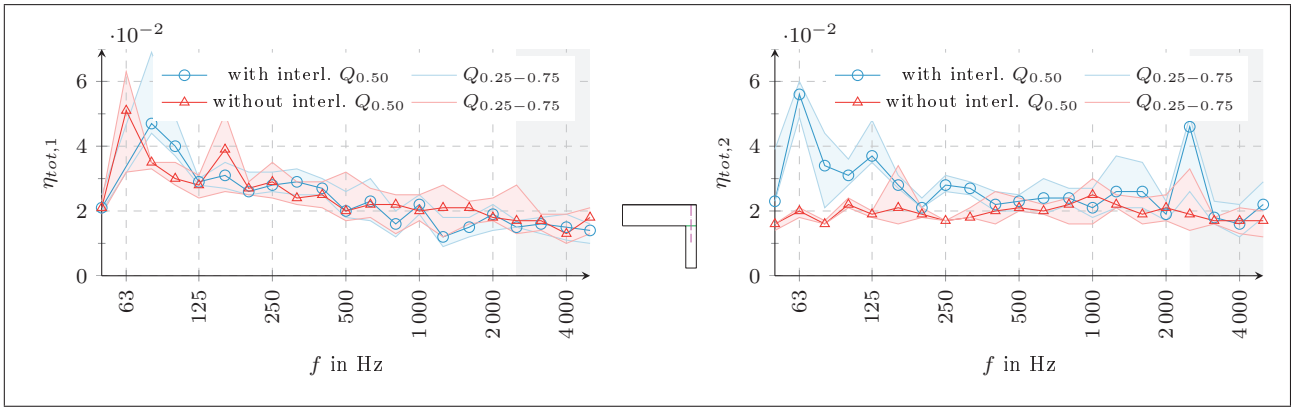

Figure 4. Quartiles of total loss factors of subsystem 1 (ceiling) and 2 (wall) of the L-shaped junction (s. fig. 3, left).

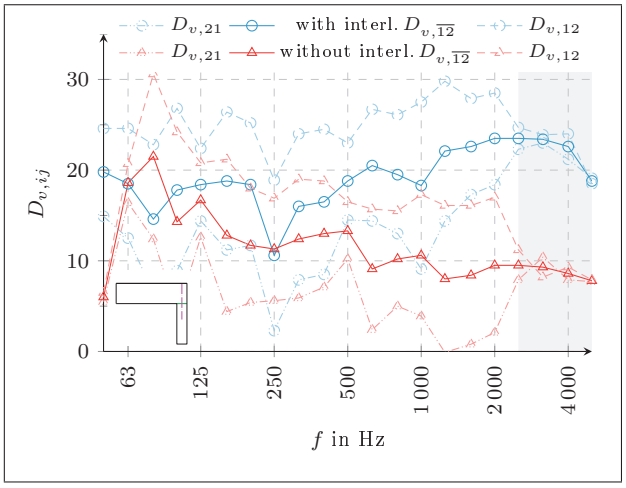

Figure 5. Effect of the resilient interlayer on velocity level difference of L-shaped junction. In the grey area the signal-to-noise ratio is $\leqslant 10\,dB$.

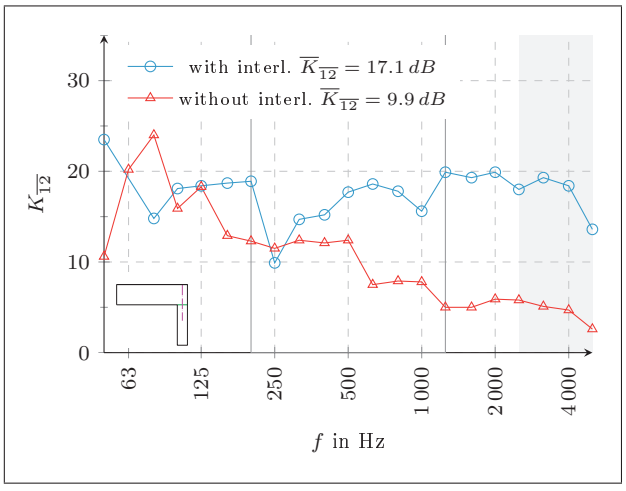

Figure 6. Effect of the resilient interlayer on vibration reduction indices of L-shaped junction (s. fig. 3, left). $\overline{K}_{\overline{ij}}$ is the arithmetic mean of $K_{\overline{ij}}(f\,\epsilon\,[200/1250]\,Hz)$. In the grey area the signal-to-noise ratio is $\leqslant 10\,dB$.

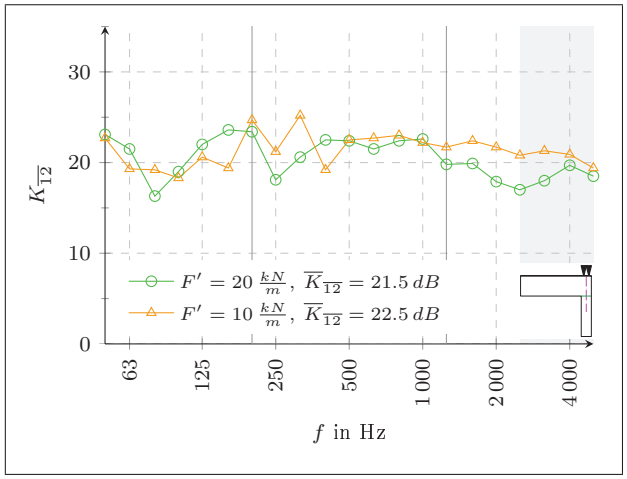

Figure 7. Vibration reduction indices of L*-shaped junction with respect to the extra load F'. $\overline{K}_{\overline{ij}}$ is the arithmetic mean of $K_{\overline{ij}}(f\,\epsilon\,[200/1250]\,Hz)$. In the grey area the signal-to-noise ratio is $\leqslant 10\,dB$.

Figure 9 shows the differences of the vibration reduction indices between the variations with and without elastic interlayers for each transfer path. The highest difference can be observed on the transfer path between the walls (subsystem 2 and 4). The difference between the two variations mounts to approx. 14 dB in the single values.

Comparing transfer path 12 to 14 the spectral behaviour as well as the single values for the vibration reduction indices are very similar in the mid and high frequency range, for both cases of with or without elastic interlayers. The effect of an increase of the vibration reduction indices using elastic interlayers is clearly observable, the difference in the single number values amount to approx. 7 to 8 dB. This does not hold for the low frequency range (below 200 Hz). There the sound transmission on path 14 of the two variations are similar. In contrast the vibration reduction indices of path 12 is higher in case of using the angle brackets with an resilient interlayer between.

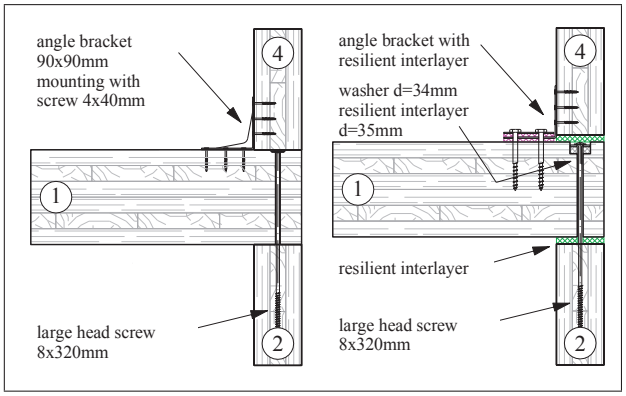

Figure 8. Variations of T-shaped junctions. In the left case (T1) no interlayer was used, in the right case (T2) with resilient interlayer between the building elements and the fasteners. The distance between two fasteners is 40 cm. [10]

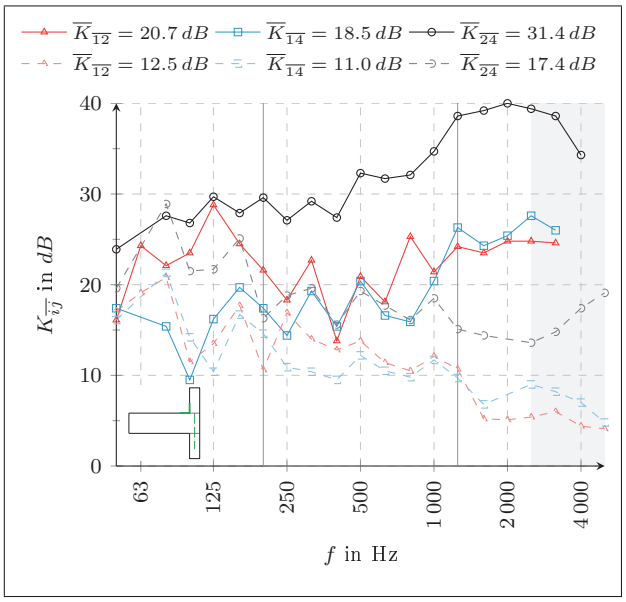

Figure 9. Vibration reduction indices of T-shaped junction without (T1: – –) and with resilient interlayer (T2: –). $\overline{K}_{ij}$ is the arithmetic mean of $K_{ij}(f\,\epsilon\,[200/1250]\,Hz)$. In the grey area the signal-to-noise ratio is $\leqslant 10\,dB$. [10]

3. Modelling with an commercial tool

The commercial software VAOne® has been used to model a rather simple SEA model for the L-shaped junction without resilient interlayer of the measured CLT building elements. The system is divided into two subsystems and the material properties of table I are used to describe the subsystems as an orthotropic material. In a first approach the damping loss factor is supposed as constant with a value of $\eta_{jj} = \eta_{ii} = 1.9\%$ for both subsystems. The modes in bands have been calculated and are shown in figure 10; above 315 Hz there are at least five modes per 1/3 octave band.

In the simple case of only two subsystems and subsystem i excited the energy balance equation can be

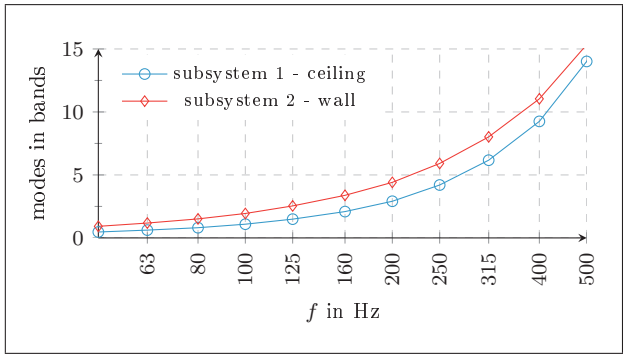

Figure 10. Modes per 1/3-octave band (flexure), calculated with VAOne®, for both subsystems setting up the L-shaped junction.

approximated [11] by equation 8 to determine η_{ij} from measurement data. In this case η_{ij} can be calculated by the ratio of the energies E of both subsystems and the total loss factor $\eta_{tot,j}$ of subsystem j.

$$\eta_{ij} = \frac{E_j}{E_i} \cdot (\eta_{ji} + \eta_{jj}) = \frac{m_j \cdot \langle \tilde{v}_j^2 \rangle}{m_i \cdot \langle \tilde{v}_i^2 \rangle}\, \eta_{tot,j} \qquad (8)$$

The calculation of the vibration reduction indices K_{ij} with η_{ij} (eq. 9) is described in a draft [12] for EN 12354. In contrast to equation 5 K_{ij} is dependent on the direction. To get an equivalent $K_{\overline{ij}}$ (s. fig. 6 and 12) the values of both directions are averaged. Comparing equation 8-9 to equation 5 additional information about masses and the coincidence frequencies f_c of both subsystems is needed.

$$K_{ij} = -10 \lg\left(\eta_{ij}\, \frac{\pi^2\, S_i}{c_0\, l_{ij}} \sqrt{\frac{f_{c,i}}{f_{c,j}}}\, \sqrt{f_{ref}\, f}\right) \qquad (9)$$

VAOne® provides different standard connections of the junctions, either a so-called line junction or point-junctions. In order to test the standardized connection types:

- Line junction (LJ)
- 2-point-junction (2PJ)
- 3-point-junction (3PJ)

For these junctions η_{ij} were calculated by VAOne® using the spatial averaged velocity level $L_{v,i}$ of the excited panel from the measurements for excitation of the equivalent subsystem in SEA-model. Figure 11 shows these results of η_{21} compared with those from experimental SEA calculated by equation 8. In the lower part of the frequency range between 315 Hz and 2500 Hz the approach with *3-point-junction* matches best η_{21} calculated from measurement data. Above 630 Hz the approach *line junction* gives better agreement. Another variation using a point junction for every screw results in a too high η_{21}. In the opposite direction the differences between simulated and calculated coupling loss factors η_{12} turned out to be even higher. The resulting direction averaged vibration reduction indices $K_{\overline{ij}}$ from (eq. 9) are presented

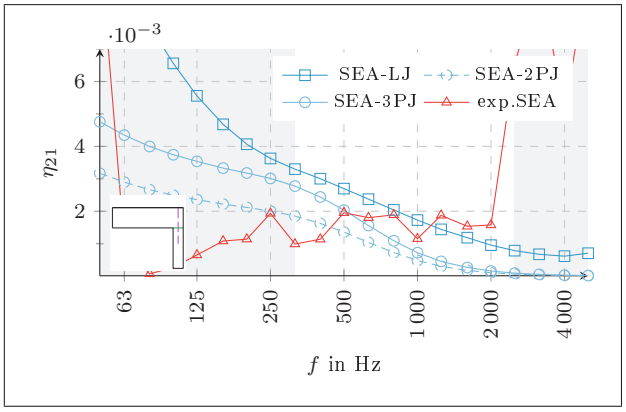

Figure 11. Coupling loss factors between subsystem 2 (wall) and 1 (ceiling) of the L-shaped junction (s. fig. 3, left). Comparison of different kinds of junctions in the SEA-model versus a calculation from measurements.

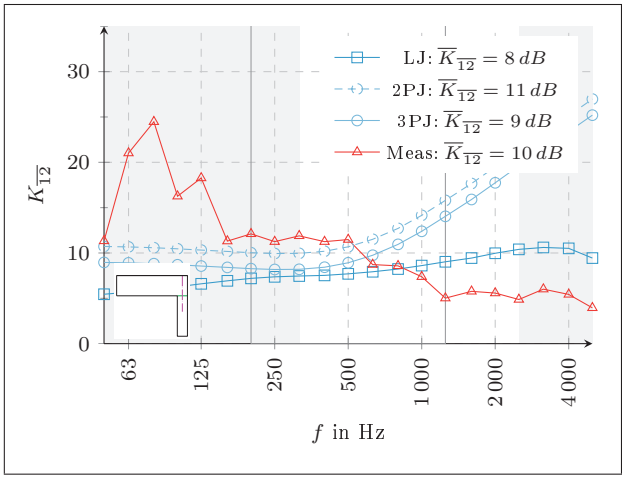

Figure 12. Vibration reduction indices of the L*-shaped junction. Comparison of different kinds of junctions in the SEA-model versus a calculation from measurements. $\overline{K_{ij}}$ is the arithmetic mean of $K_{ij}(f\,\epsilon\,[200/1250]\,Hz)$. In the left grey area the number of modes is less than five in the 1/3-octave bands. In the right grey area the signal-to-noise ratio is $\leqslant 10\,dB$.

in figure 12. A combination of *3-point-junction* in the lower and *line junction* in higher frequency domain obviously leads to an acceptable agreement with measurement data; at least the singe number values are in the right ballpark.

4. CONCLUSIONS

Vibration reduction indices for various junctions of CLT elements have been measured. The results are in good agreement with values measured by different groups; for a short survey see [1]. The junctions were modified using elastic interlayer between the junctions. This measure showed a clear impact on the vibration reduction index. A calculation of the vibration reduction indices by using coupling loss factors η_{ij}, resulting from a SEA-model show a fair agreement. Further steps of the modelling are necessary to verify these findings and to model junctions with interlayer.

Acknowledgement

The results are based on the current status of the research project *Vibroacoustics in the planning process for timber constructions* funded by the German Research Foundation (DFG) and German Federation of Industrial Research Associations (AIF). It is carried out by Technical University Munich, ift Rosenheim and University of Applied Sciences Rosenheim.

References

[1] A. Rabold et al. “SEA based prediction for integrated vibroacoustical design optimization of multi-storey buildings”. In: *Euronoise*. 2015.

[2] S. Mecking. “Bauteilstöße im Holzmassivbau - Messtechnische Bestimmung von Eingangsgrößen für eine Schallschutzprognose”. Masterarbeit. Hochschule Rosenheim, 2014.

[3] A. Gülzow. “Zerstörungsfreie Bestimmung der Biegesteifigkeit von Brettsperrholzplatten”. Dissertation. ETH Zürich, 2008.

[4] S. Schoenwald et al. “Sound insulation performance of Cross Laminated Timber Building Systems”. In: *Internoise*. 2013.

[5] M. Kohrmann et al. *Planungshilfen zur schall- und schwingungstechnischen Beschreibung von Holzdecken und zur Bewertung udn Dimensionierung von angepassen Schwingungsschutzsystemen: Abschlussbericht zum AiF Forschungsvorhaben VibWood*. 2014.

[6] C. Winter et al. “Modelling the Sound Transmission across Junctions of Building Components by Energy Influence Coefficients”. In: *EURODYN*. 2014.

[7] E. Gerretsen. “Vibration Reduction Index Kij , a new Quantity for Sound Transmission at Junctions of Building Elements”. In: *Internoise*. 1996, pp. 1475–1480.

[8] DIN EN ISO 10848-1. *Akustik - Messung der Flankenübertragung von Luftschall und Trittschall zwischen benachbarten Räumen in Prüfständen*. Berlin, 2006.

[9] M. Schramm. “Vertikale Flankenübertragung bei Holzmassivdecken”. Diplomarbeit. Hochschule Rosenheim, 2008.

[10] T. Kruse. “Messtechnische Untersuchung zur Stoßstellendämmung und Ausbreitungsdämpfung von Brettsperrholzbauteilen”. Bachelorarbeit. Hochschule Rosenheim, 2015.

[11] R. J. M. Craik. “The prediction of sound transmission through buildings using statistical energy analysis”. In: *J Sound Vib* 82.4 (1982), pp. 505–516.

[12] prEN 12354-1. *Building Acoustics - Estimation of acoustic performance of buildings from the performance of elements: Part 1: Airborne sound insulation between rooms*. 2013.